Inorganic Chemistry

Article

pubs.acs.org/IC

2,2′-Pyridylpyrrolide Ligand Redistribution Following Reduction

Keith Searles, Atanu K. Das, René W. Buell, Maren Pink, Chun-Hsing Chen, Kuntal Pal, David Gene Morgan, Daniel J. Mindiola, and Kenneth G. Caulton*

Department of Chemistry, Indiana University, Bloomington, Indiana 47405, United States

Supporting Information

ABSTRACT: The potential redox activity of the 2,2′-pyridylpyrrolide ligand carrying two CF_3 substituents (L^2) is investigated. Synthesis and characterization of d^6 and d^7 species $M(L^2)_2$ for M = Fe and Co are described (both are nonplanar, but not tetrahedral), as are the Lewis acidity of each. In spite of CV evidence for quasireversible reductions to form $M(L^2)_2^{q-}$ where q = 1 and 2, chemical reductants instead yield divalent metal complexes $KM(L^2)_3$, which show attractive interactions of K^+ to pyrrolide, to F, and to lattice toluene π cloud. The collected evidence on these products indicates that pyridylpyrrolide is a weak field ligand here, but CO can force spin pairing in $Fe(L^2)_2(CO)_2$. Evidence is presented that the overall reductive reaction yields 33 mol % of bulk metal, which is the fate of the reducing equivalents, and a mechanism for this ligand redistribution is proposed. Analogous ligand redistribution behavior is also seen for nickel and for trimeric monovalent copper analogues; reduction of $Cu(L^2)_2$ simply forms $Cu(L^2)_2^-$.

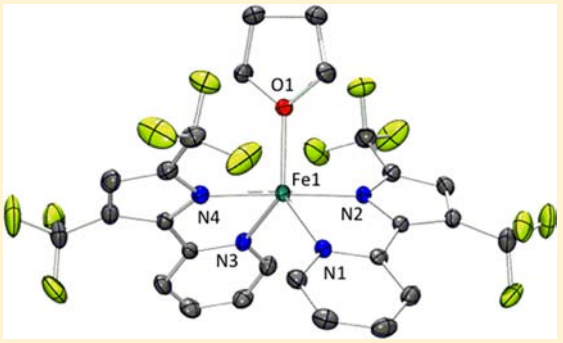

INTRODUCTION

We have been attempting to utilize pyridylpyrrolide ligands, L^n below, as potential redox auxiliaries

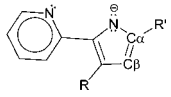

L^n

	R	R'
n = 2	CF_3	CF_3
1	CF_3	^{t}Bu
0	^{t}Bu	^{t}Bu

or redox noninnocent ligands, in later transition metal chemistry. The idea is that the pyrrolide ligand alone is electron rich, thus stabilizing high oxidation state complexes by π donation, but also increasing the overall reducing power of its lower valent metal complexes. The partnered pyridyl motif was thought to be susceptible to being reduced by acceptance of electrons into its π^* orbital, hence sharing any reduction which might classically have targeted simply reduction of the metal alone. Studies of bipyridyl ligands over the decades have certainly shown[1−8] that this ligand can be reduced to mono- and dianionic states. Pyridylpyrrolide, tunable via its ring substituents,[9,10] was thus envisioned as a push−pull ligand, subject to redox activity under either oxidative or reductive conditions. Push/pull character is a feature not present in other explored redox-active ligands; this characteristic increases the versatility of their complexes to being both oxidizable and reducible. They can be reducing agents and oxidants, respectively. For example, DFT calculation (Figure 1) of *N*-methyl pyridyl-pyrrolide (to have no redox-active metal present) shows that the LUMO is primarily pyridyl (hence the site of reduction) and the HOMO is primarily pyrrolide (hence the site of oxidation).

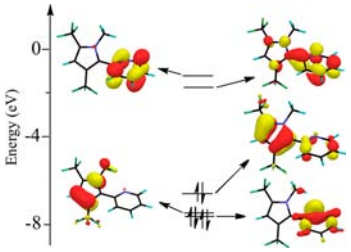

Figure 1. Frontier orbitals of the *anti* conformer of *N*-methyl 3,5-$(CF_3)_2$-2,2′-pyridylpyrrolide, showing two occupied orbitals having pyrrolide character and two unoccupied having pyridyl character.

We report here the synthesis of new $M(L^2)_2$ complexes (M = Fe and Co) and a more general survey of the reactions of these, as well as $Ni(L^2)_2$, with alkali metal reductants, to compare the reducibility along the d^6, d^7, d^8 series. As will be seen, the story will take a different path due to the active participation of ligand redistribution and disproportionation of the primary reduced product, $M(L^2)_2^{q-}$. One sometimes reads statements, following attempted reductions by magnesium or potassium, such as "In all cases, however, only intractable mixtures of products were obtained."[11] The present report may shed light on some of these problems.

Received: April 3, 2013
Published: April 19, 2013

   dx.doi.org/10.1021/ic400803e | *Inorg. Chem.* 2013, 52, 5611−5619

RESULTS

Iron. Reaction of KL^2 with anhydrous $FeCl_2$ (2:1 mol ratio) in THF at 25 °C occurs first with color change to orange, then slower to yellow to give a solution from which yellow solid was isolated by filtration, and purified by washing with pentane. The ^1H NMR spectra of this product depends on how long the solid has been subjected to vacuum, suggesting variable amounts of THF coordinated to iron in a rapidly established equilibrium between $Fe(L^2)_2$ and its THF adduct; judging by the range of chemical shifts, the molecules are paramagnetic. The NMR spectra[12] show five signals for the ring protons of L^2, two for coordinated THF, and two for CF_3; it is possible to use very short FT acquisition times because of the paramagnetism, and hence obtain spectra with extremely good *S*/*N* ratio, even for broad signals. Even in THF solvent, the spectra show paramagnetism, with one ^1H NMR spectral signal being much broader than the other four. Depending on sample history (time in vacuum, dilution of sample), one of the two ^{19}F NMR chemical shifts is highly variable. All of this is consistent with solution population of both $Fe(L^2)_2(THF)$ and $Fe(L^2)_2$, with rapid exchange averaging of corresponding signals in the two species. An Evans method magnetic susceptibility determination at 25 °C in THF (to ensure full equilibrium formation of the THF adduct) yielded a value of 5.2 Bohr magnetons, which is consistent with four unpaired electrons per iron. Mass spectra show $Fe(L^2)_3^-$ in the negative ion APCI mode, but positive ion APCI spectra show no metal-containing species. Yellow crystals were grown by slow evaporation from a concentrated pentane solution, and were shown (Figure 2) by single crystal X-ray diffraction to be $Fe(L^2)_2(THF)$, with a trigonal bipyramidal structure with the two pyrrolide nitrogens being axial. Intraligand bond lengths show the two L^2 ligands to be equivalent, and consistent with a charge state $(L^2)^{1-}$. The THF oxygen is coplanar with its three substituents. The two rings within a given L^2 ligand have dihedral angles of less than 9°, and thus are essentially coplanar.

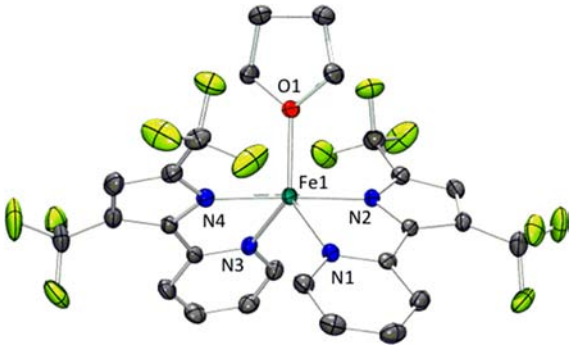

Figure 2. ORTEP drawing (50% probability) of the nonhydrogen atoms of $Fe(L^2)_2(THF)$, showing selected atom labeling. Unlabeled atoms are carbons, or, if terminal, are F of the CF_3 groups. Selected structural parameters follow (Å, deg): Fe1–O1, 2.0769(12); Fe1–N1, 2.1163(14); Fe1–N2, 2.1123(13); Fe1–N3, 2.1177(13); Fe1–N4, 2.1033(14); O1–Fe1–N1, 126.10(5); O1–Fe1–N2, 91.20(5); N1–Fe1–N2, 77.33(5); O1–Fe1–N3, 127.75(5); N1–Fe1–N3, 106.15(5); N2–Fe1–N3, 101.05(5); O1–Fe1–N4, 91.10(5); N1–Fe1–N4, 101.02(5); N2–Fe1–N4, 177.67(5); N3–Fe1–N4, 77.78(5); Fe1–O1–C23, 124.40(9); Fe1–O1–C26, 125.90(10); C23–O1–C26, 109.69(12).

DFT calculation on $Fe(L^2)_2(THF)$ in spin states S = 0, 1, and 2 (the latter two unrestricted calculations) showed the highest spin state to be most stable. Spin state has its largest geometric effect on Fe–N bond distances, and all these are longest for S = 2. The calculated Fe–N bond distances are in best agreement with the experimental ones for the S = 2 state, providing further support for the experimental spin state determination. In this spin state, 95% of the spin is on the iron, consistent with little ligand orbital participation in the SOMOs of this species.[12] Regarding *reduction* of this S = 2 species, examination of its LUMO (166β) shows it to be a mixture of d orbitals (mostly of $d_{x^2-y^2}$ character) with the π orbitals of the pyridyl groups. HOMO (β165) is a nonbonding metal d_{xz} orbital; thus, one electron *oxidation* should cause oxidation at Fe of $Fe(L^2)_2(THF)$, to create Fe(III).

Treatment of $Fe(L^2)_2(THF)$ with vacuum for 24 h at 25 °C gives clean conversion to a pale red compound which retains one THF molecule for each *two* Fe atoms. This appears to be evidence that iron here is quite reluctant to convert completely to $Fe(L^2)_2$, which would have 14 valence electrons. Both the ^1H and ^{19}F NMR spectra of this new product and of $Fe(L^2)_2(THF)$ are distinguishable, and integration of L^2 versus THF protons agrees with the retention of approximately one THF for every two iron ions. Attempts to grow crystals of the di-iron species $Fe_2(L^2)_4(THF)$ were unsuccessful from either pentane or toluene.

To test for possible bis-adduct formation, $Fe(L^2)_2(THF)$ was reacted with CO (1 atm). This gives modest color change from yellow to dark yellow and full conversion to $Fe(L^2)_2(CO)_2$, with only one isomer formed, that with the carbonyls *cis*. The CO stretching frequencies, 2088 and 2044 cm^{-1}, show the modest electron richness in this $Fe(L^2)_2$ moiety. For comparison, the CO frequencies for *cis*-$Fe(Me_2dithiocarbamate)_2(CO)_2$ are[13] 2090 and 2040 cm^{-1} while those for a very electron donating divalent iron amidinate analogue are 1999 and 1929 cm^{-1}.[14] Vacuum treatment does not cause loss of CO at 25 °C, showing tight binding of these ligands. The spectra do not conclusively establish whether both pyrrolide nitrogens are *cis* or *trans*, but the NMR spectra of this diamagnetic product prove C_2 symmetry. DFT geometry optimization calculations[12] yielded the C_2 symmetric species, and show that the *cis* dicarbonyl structure with pyrrolide nitrogens mutually *trans* is 12.7 kcal/mol more stable than that with pyrrolide nitrogens mutually *cis*.

Cobalt. Reaction of anhydrous $CoCl_2$ with KL^2 (1:2 mol ratio) in THF occurs to completion over 18 h at 25 °C to produce a yellow green solution from which green solid can be isolated by vacuum removal of volatiles after filtration. NMR spectra of this green solid in THF shows two paramagnetically shifted ^{19}F NMR signals, of which one is significantly broader, and five signals in the ^1H NMR spectrum, with one signal broader than the other four. These data are consistent with a single environment of L^2 in a species $Co(L^2)_2(THF)_n$. Exposure of the green solid to vacuum for greater than approximately 4 h results in a mixture of green and red brown solids. Thus, coordination of THF is anticipated, and full conversion to the red-brown solid can be accomplished by dissolving the green solid in benzene and removing volatiles in vacuum. NMR spectra of this red-brown compound in benzene show no evidence for signals of THF, but show two different paramagnetically shifted ^{19}F NMR signals, of equal intensity, and five new signals in the ^1H NMR spectrum, consistent with only one environment for an L^2 ligand, hence a species without the coordination of THF. Only one of the ^1H NMR signals is significantly broader than the other four. Crystals grown by

dx.doi.org/10.1021/ic400803e | Inorg. Chem. 2013, 52, 5611–5619

cooling a saturated solution of toluene to −37 °C were shown (Figure 3) by single crystal X-ray diffraction to be $Co(L^2)_2$ with

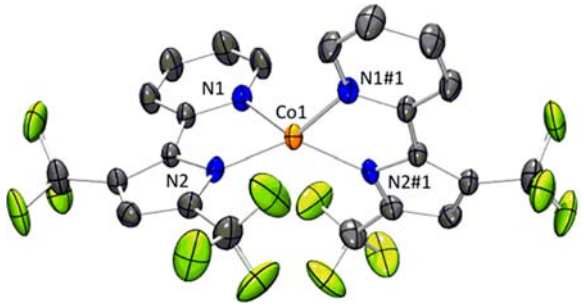

Figure 3. ORTEP drawing (25% probability) of the nonhydrogen atoms of $Co(L^2)_2$, showing selected atom labeling. Unlabeled atoms are carbons, or, if terminal, are F of the CF_3 groups. The molecule has crystallographic C_2 symmetry. Selected structural parameters (Å, deg): Co1−N2, 1.981(6); Co1−N1, 2.041(7); N2−Co1−N2#1, 135.5(6); N2−Co1−N1, 81.5(3); N2−Co1−N1#1, 120.3(3); N1−Co1−N1#1, 123.6(6).

rigorous C_2 crystallographic symmetry. The four coordinate structure is neither planar nor tetrahedral, but is perhaps best described as compressed tetrahedral. The angle between the pyrrolide nitrogens is larger (135.6°) than that between the pyridyl nitrogens (123.6°). The distances within the L^2 ligand are identical, within one esd, for the iron and cobalt analogues, showing that there is no difference in the electronic structure of the ligand between these two metals. An Evans method magnetic susceptibility determination in benzene shows a magnetic moment of 4.2 Bohr magnetons, consistent (compared to other cobalt complexes)[15−17] with the presence of 3 unpaired electrons, and the APCI mass spectrum shows $Co(L^2)_2^+$ in the positive ion spectrum and $Co(L^2)_3^{-1}$ in the negative ion spectrum. Thus, ligand redistribution is an efficient process in the ionization chamber.

We surveyed the Lewis acidity of $Co(L^2)_2$ by simply noting the color change which occurs from red-brown to green upon adding Lewis bases in benzene. This was observed with acetone, benzonitrile, and THF. In contrast, there was no evidence for adduct formation under 1 atm CO, or, remarkably, O_2. In the case of benzonitrile and THF, we characterized the adduct formation by alteration of the ^1H and ^{19}F NMR spectra after color change. In the case of benzonitrile, at a mole ratio of 1/30 Co/nitrile, we observe growth of five new ^1H NMR chemical shifts and two ^{19}F NMR signals characteristic of an adduct. By the different means needed to remove THF from the iron and cobalt compounds, we conclude that the iron example is the stronger Lewis acid.

Exploration of Redox Activity. *Cyclic Voltammetry.* Cyclic voltammetric studies on $M(L^2)_2(THF)$ for M = Fe and Co were carried out at a platinum electrode in THF with 0.3 M $[n\text{-}Bu_4N][PF_6]$ supporting electrolyte (Figures 4 and 5). Both

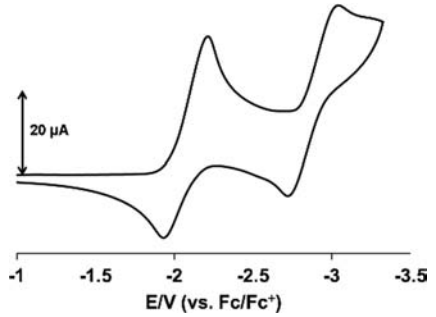

Figure 5. Cyclic voltammogram of $Co(L^2)_2(THF)$ in THF/0.3 M $[n\text{-}Bu_4N]PF_6$ at 25−175 mV s^{-1}.

complexes show two quasireversible reductions occurring at −2.03 and −2.36 V versus Fc^+/Fc (referenced at 0.0 V) for Fe and −2.07 and −2.88 V versus Fc^+/Fc for Co. The first reduction potential of $Co(L^2)_2(THF)$ occurs at a similar potential to that of the Fe analogue. The second reduction of Co is 520 mV higher than that of Fe.

Following this reasoning, it was expected that if oxidations could be observed, the oxidation potential for the Co compound should occur at a lower potential than that of the Fe compound. However, only the $Fe(L^2)_2(THF)$ shows a quasireversible oxidation (Figure 4). No oxidation can be observed out to 0.57 V in the CV for the Co compound. Since normally both Fe(III) and Co(III) are relatively accessible oxidation states, it was surprising to see no oxidation for the Co complex, although these do agree with the fact that $Fe(L^2)_2(THF)$ is extremely air sensitive while the Co compound is not. The inaccessibility of $Co(L^2)_2^+$ by outer sphere electron transfer is surprising, as is the complete lack of reaction of $Co(L^2)_2$ with O_2.

We also wanted to extend our comparison to later transition metals. The CV of 18 valence electron $Ni(L^2)_2(THF)$ under the same conditions (e.g., in THF) shows two quasireversible reductions at −1.52 and −2.24 V versus Fc^+/Fc. Considering that the doubly reduced compound is a 20 valence electron complex, the potentials for both reductions are modest compared to the fully reduced Fe (18 electrons) and Co (19

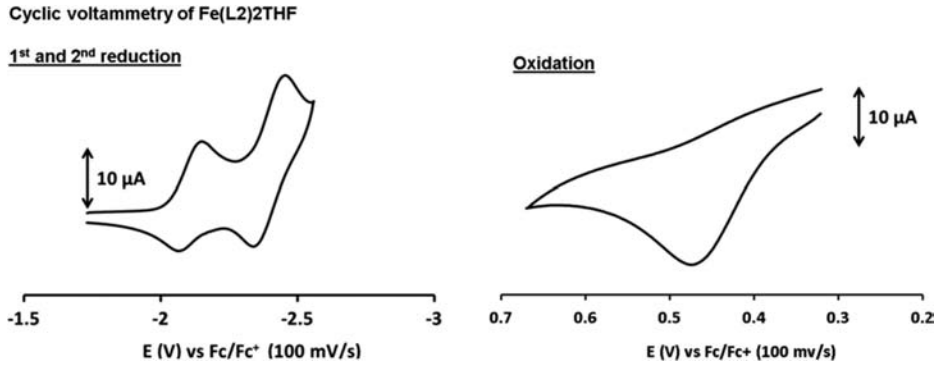

Figure 4. Cyclic voltammogram of $Fe(L^2)_2(THF)$ in THF/0.3 M $[n\text{-}Bu_4N]PF_6$ at 250 mV s^{-1} (left, cathodic scans; right, anodic scans).

dx.doi.org/10.1021/ic400803e | Inorg. Chem. 2013, 52, 5611−5619

electrons) reduction potentials. It is noteworthy that, of the three metals, the Ni compound has the most valence electrons, but also has the least negative reduction potential. The Ni compound exhibits no features in the CV characteristic of oxidation, and of the three complexes (Fe, Co, and Ni), only the lowest valence electron count Fe compound is capable of being oxidized. Since all of the compounds, containing two potentially noninnocent ligands, show two reduction waves, we felt that chemical reductions warranted investigation to establish the locus of the added electron.

Reactions with Alkali Metals. *Iron.* Reduction of $Fe(L^2)_2$ with excess KC_8 or Na in THF or Et_2O proceeds over 3 h with color change to orange-red, after removal of graphite, in the case of KC_8. This product shows 15 proton chemical shifts and six ^{19}F chemical shifts,[12] which we take to indicate (at least) *three* inequivalent L^2 units per species; the range of proton chemical shifts (128 ppm) shows the product to be paramagnetic. Crystals grown from toluene/pentane were shown (Figure 6) to be of composition (toluene)$KFe(L^2)_3$, which exists in the solid state as a weakly associated dimer (Figure 7). The iron complex has a *mer*-$Fe(L^2)_3$ environment (see below for a comparative discussion of the MN_6 distances), in full agreement with no symmetry for the anion and thus the large number of chemical shifts. The K^+ interacts as a π complex with all five atoms of one pyrrolide and several atoms in a second pyrrolide,[18−22] but also coordinates to two adjacent carbons of the toluene. Finally K^+ interacts with one CF_3 fluorine of a second $KFe(L^2)_3$ complex to create a centrosymmetric dimer. Even if the K^+ interaction with pyrrolide is lost (e.g., by solvation) or if K^+ migrates fast among all three L^2 chelates in solution, the underlying *mer* stereochemistry at Fe maintains the symmetry inequivalence of the three L^2. This product is thus not the result of a redox change of the ligand, but instead a pyridylpyrrolide ligand redistribution. The product anion is an 18 electron species, and proves the Lewis acidity (14 valence electron count) of $Fe(L^2)_2$ itself. There is clearly *no* steric crowding in $Fe(L^2)_2$ that prevents binding of an additional bidentate ligand.

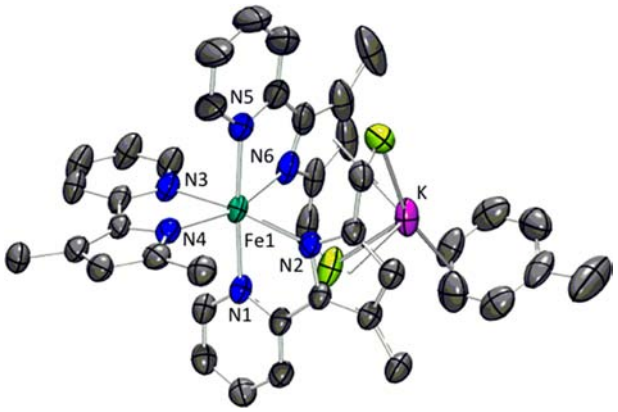

Figure 6. ORTEP view (50% probabilities) of $[KFe(L^2)_3]\cdot$(toluene) with hydrogen (and some fluorines) omitted for clarity. Unlabeled atoms are carbons or fluorines, and the K-η^5-pyrrolide ligand involves N2. Selected structural parameters (Å, deg): Fe1−N4, 2.156(3); Fe1−N5, 2.164(3); Fe1−N1, 2.166(3); Fe1−N6, 2.179(3); Fe1−N2, 2.214(3); Fe1−N3, 2.223(3); N5−Fe1−N1, 175.38(10); N4−Fe1−N6, 161.76(10); N2−Fe1−N3, 169.57(10).

The cyclic voltammogram[12] of complex $KFe(L^2)_3$ in THF shows no reduction wave down to −2.5 V, and one reversible oxidation, at −0.25 V (both vs Fc^+/Fc), the latter consistent with formation of a chemically persistent neutral $Fe(L^2)_3$ species; the low potential for oxidation may be related to the anionic charge of the complex, as well as accessibility of Fe(III) in a tris pyrrolide environment. The absence of reduction is perhaps due to the 18 electron configuration, as well as the overall negative charge.

Evans method magnetic susceptibility determination for $KFe(L^2)_3$ in benzene at 25 °C gave a value of 5.1 Bohr magnetons, consistent with four unpaired electrons for this d^6 species. This means that overall splitting of the five d orbitals is not high enough to overcome the spin pairing energy penalty and in particular that the z^2 and $x^2 - y^2$ orbitals are both singly occupied.

The production of a 3/1 L^2/Fe complex from reaction with reducing agents implies formation of iron metal. We sought support for this by powder XRD[12] and indeed detected FeO (oxidation during sample handling), and also detected iron particles by microscopic examination of the insoluble reaction

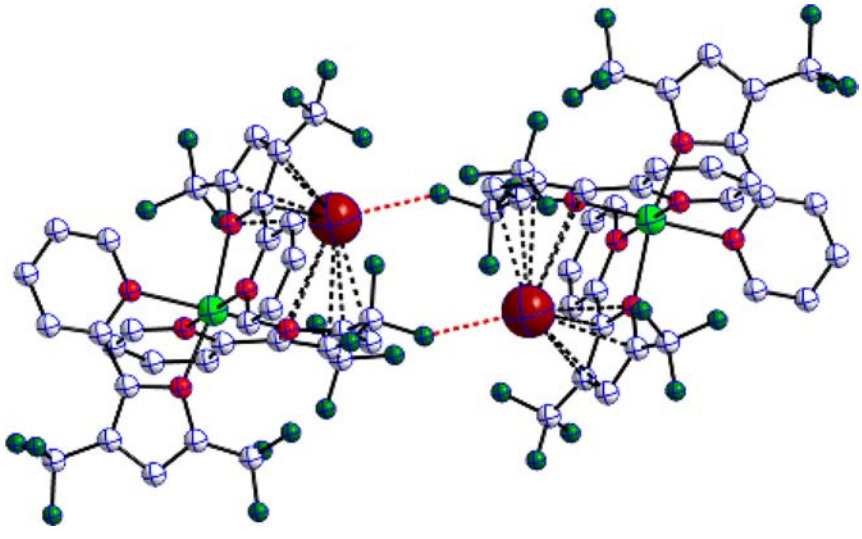

Figure 7. Solid state dimerization of $[KFe(L^2)_3]\cdot$(toluene), showing intermolecular K/F interactions.

dx.doi.org/10.1021/ic400803e | *Inorg. Chem.* 2013, 52, 5611−5619

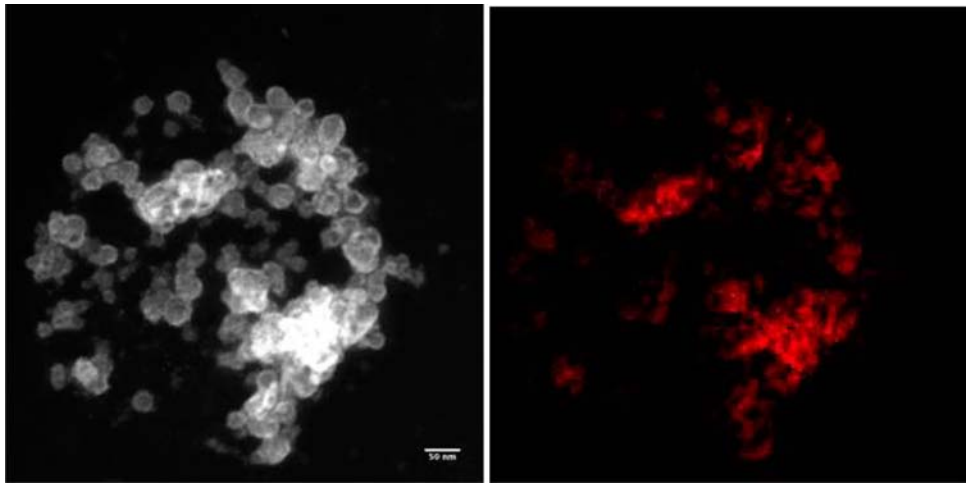

Figure 8. STEM dark field image (left) and false color energy dispersive spectroscopy map of iron in the same area, for insoluble residue from KC_8 reduction of $Fe(L^2)_2$. Scale bar shows 50 nm.

residue using energy-dispersive X-ray spectroscopy (EDX, Figure 8).

Attempts to capture the reduction product $Fe(L^2)_2^-$ by reduction of $Fe(L^2)_2$ with sodium, or KC_8 [mole ratio Fe/K = 1/2.2] in Et_2O or THF by chemical trapping under 1 atm of N_2, or of CO_2 or of H_2 all failed, providing only $MFe(L^2)_3$ with M = Na or K as the only detectable metal complex.

Cobalt. Reduction of brown-red $Co(L^2)_2$ with KC_8 (mole ratio1:0.67) in THF proceeds within minutes with color change to yellow after separation of graphite. The ^1H NMR spectrum of the product shows 14 chemical shifts, one of which is likely too broad to observe, that are all nicely resolved and reasonably sharp over a chemical shift range of ~150 ppm.[12] This is the number of protons in *three* L^2 ligands, and suggests three inequivalent ligands in the product. Fully consistent with that conclusion is the observation of six ^{19}F NMR chemical shifts. Moreover, KL^2 was found to react with $Co(L^2)_2$ in THF to form this same product, indicative of the (nonredox) Lewis acidity of the $Co(L^2)_2$ species. Attempts to isolate the product as a powder by removal of solvent under reduced pressure yields KL^2 and $Co(L^2)_2$. Thus, to obtain single crystals of $[KCo(L^2)_3]\cdot$(toluene) the above reaction had to be performed in toluene. After filtering the reaction mixture through Celite to remove graphite, pentane was layered on the toluene solution, and the reaction mixture was cooled to −35 °C resulting in the formation of single crystals.

The crystal structure shows that the cobalt product (Figure 9) has formula $KCo(L^2)_3$(toluene), just as the iron compound discussed above, but the two are not crystallographically isomorphous. Again, the pyridylpyrrolide ligands coordinate to the metal in a distorted octahedral geometry with the ligands occupying a *meridional* geometry, and again, the K^+ interacts with the π-system of two pyrrolides, one η^3-coordination and the other interacting in an η^5-coordination, as well as with the toluene π cloud.

The first coordination sphere of both $KM(L^2)_3$(toluene) structures (Scheme 1) show the pyrrolides to be orthogonal, which minimizes their π-conflict with d orbitals. In both, the MN_6 distances show C_2 symmetry which an all-monodentate *mer*-MN_6 species would have. In general, corresponding distances are ~0.03 Å shorter for cobalt. Both MN_6 substructures have an idealized C_2 axis, containing the central pyrrolide and pyridine, along which Co/N distances are longer than on the other two octahedral axes. The origin of this axial elongation is attributed to that pyrrolide interacting with the K^+ in a η^5-fashion, decreasing its nucleophilicity. Certainly the elongation is not a Jahn−Teller effect (which is not rigorously predicted for a *mer* structure), and it is not a traditional *trans* effect, which would shorten the bond trans to a longer bond.

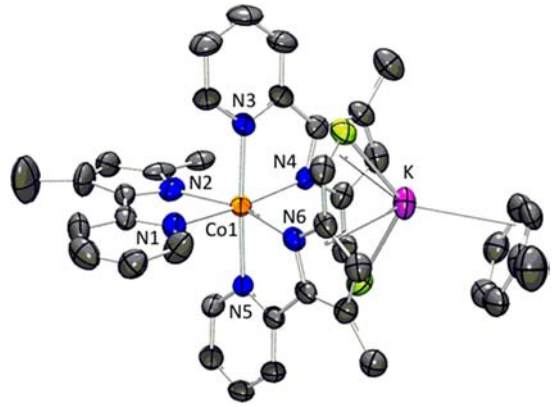

Figure 9. ORTEP view (50% probabilities) of $[KCo(L^2)_3]\cdot$(toluene) with hydrogen and some fluorines omitted for clarity. Unlabeled atoms are carbons or fluorines (green), and the K-η^5-pyrrolide ligand involves N4. Selected structural parameters (Å, deg): Co1−N5, 2.120(4); Co1−N3, 2.126(4); Co1−N2, 2.141(5); Co1−N6, 2.149(4); Co1−N4, 2.179(4); Co1−N1, 2.229(5); N5−Co1−N3, 176.37(15); N2−Co1−N6, 161.08(17); N4−Co1−N1, 172.62(15).

Scheme 1. Comparison of M−N distances (Å) for M = Fe (red, italic) and M = Co (black)[a]

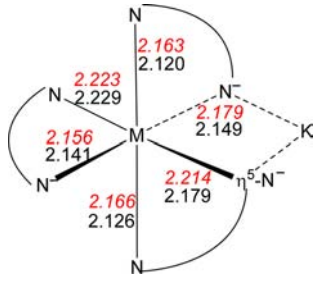

[a] N^- represents the pyrrolide moiety.

dx.doi.org/10.1021/ic400803e | *Inorg. Chem.* 2013, 52, 5611−5619

Finally, from these structures, it is not possible to generalize that an anionic nitrogen always binds shorter (or longer) than a pyridyl nitrogen.

This cobalt structure shows the generality of the composition and structure of that already described for iron. Noncovalent Fe/Co differences are less important than their similarities, and occur at these latter weak interactions. The weaker of the interactions in both the iron and cobalt analogues, that between K^+ and one C−F fluorine (green in Figure 9), are intramolecular. In summary, the need to satisfy electrophilic K^+ with even unusual interactions arises from our intentional absence of better donors such as ethers.

As with iron, production of $KCo(L^2)_3$ implies a reduction product, which was established to be cobalt particles within the graphite matrix using energy-dispersive X-ray spectroscopy.[12]

Reduction of $Co(L^2)_2$ using less KC_8 than 1:0.67 mol ratio does not give any different product (e.g., does not avoid cobalt metal), but gives only a reduced yield of $KCo(L^2)_3$ together with recovered $Co(L^2)_2$. Conversely, excess KC_8 decreases the yield of $KCo(L^2)_3$.

Given the complexation of potassium by the pyrrolide in the structure of KML_3 (even in the structure of KL^2, such π complexation occurs[10]), we hypothesized that this interaction was responsible for removal of the chelate from the transition metal, even in THF solvent. It must be recognized that chemical quasireversibility we observe in CV might be related to the absence of electrophilic cations, and the abundance of relatively unreactive n-Bu_4N^+ cations, as well as the shorter time scale. We speculated that ligand redistribution might be avoided by use of a reducing agent whose oxidation product was not a Lewis acid. To test for any influence of alkali metal cations, we considered outer sphere electron transfer reductants. We find that Cp_2Co does not prevent ligand redistribution, but instead yields a species with chemical shifts only modestly altered from those of $KCo(L^2)_3$, a change we attribute to the influence of a different and noninteracting Cp_2Co^+ cation.

Nickel. Reduction of $Ni(L^2)_2(THF)$ occurs in both benzene and THF; KC_8, Cp_2Co, and sodium metal are all effective reductants. The product solution is orange-brown after removal of graphite, and paramagnetic. The ^{19}F NMR spectrum[12] shows five signals, one with (accidental) double intensity, which we attribute to (cation)$Ni(L^2)_3$. The product of reaction of $Ni(L^2)_2(THF)$ with KL^2 in THF is this same $KNi(L^2)_3$. An Evans method magnetic susceptibility experiment at 25 °C in benzene shows a value of 2.74 Bohr magnetons for $KNi(L^2)_3$, which corresponds to two unpaired electrons, indicating that no reduction has occurred in forming this product. Because equimolar *para*-dimethylaminopyridine (DMAP) displaces THF (even in neat THF solvent), an attempt was made to block chelate ligand redistribution by first forming $Ni(L^2)_2(DMAP)$ in THF, then adding KC_8 (1:1 mol ratio); this gave no reduction product after 3 days at 25 °C.

Monovalent Copper. Monovalent copper offers an inquiry into reduction at L^2 because there is no molecular compound of zerovalent copper. The idea of storage of electrons in the L^2 ligand is thus what motivated study of the reaction of KC_8 with $(CuL^2)_3$;[9] we envisioned at least production of the trimer $(CuL^2)_3^-$ where the added electron might be delocalized over the three coppers, including at their appended bidentate ligands. In fact, the yellow-orange product of KC_8 (or also Cp_2Co) reaction with $(CuL^2)_3$ in arene solvent (1.25:1 mol ratio) has ^1H and ^{19}F NMR spectra in the diamagnetic chemical shift region.[12] The ^1H NMR spectrum shows a singlet, two doublets, and two triplets; the ^{19}F NMR shows two singlets. The molecule is thus C_2 symmetric, and we believe it to be $KCu(L^2)_2$. Our previous DFT[10] calculations showed that the minimum energy geometry of the anion $Cu(L)_2^{1-}$ has near-dissociation of one pyridyl from the copper, indicative that copper is quite content with coordination number less than four. We therefore tested, by a low temperature NMR study, the possibility that our room temperature NMR evidence on $KCu(L^2)_2$ was time-averaged. Proton and fluorine NMR spectra recorded at −50 °C in toluene shows no decoalescence, which might have indicated less than C_2 symmetry for $Cu(L)_2^{1-}$, so both ligands seem η^2 coordinated, leaving Cu^I four coordinate. Assembly of two ligands at one copper is mechanistically facile (e.g., intramolecular) from the trimer, since the trimer has L^2 occupying bridging sites, hence each interacting with two coppers. However, material balance (and the persistence of monovalent copper in the isolated product) indicates that the balanced reaction must be eq 1, and indeed the reaction also plates metallic copper onto the glass flask surface.

$$2(CuL^2)_3 + 3K \rightarrow 3KCu(L^2)_2 + 3Cu \quad (1)$$

We have already noticed[9] that the ion produced under mass spectrometry conditions from trimeric $(CuL^2)_3$ is $Cu(L^2)_2^+$. This suggests that ligand redistribution is a preferred path to ions among L^2 complexes of later 3d metals. New mass spectra collected for this work further supports that idea. $KCu(L^2)_2$ shows, in its APCI negative ion spectrum, $Cu^I(L^2)_2^-$; $(L^2)^-$ is also observed, showing the stability of this anion.

Divalent Copper. The yellow-orange product of 1:1 mol ratio KC_8 reaction with dark blue $Cu(L^2)_2$ (quantitative yield, based on Cu, in 10 min at 25 °C) has ^1H and ^{19}F NMR spectra in the diamagnetic chemical shift region which are indistinguishable from those of $KCu(L^2)_2$ synthesized above.[12] This is a product of reduction of copper, but apparently, finally at d^{10} copper, there is no longer demand for forming a tris-chelate complex, $Cu(L^2)_3^{2-}$. Nonredox synthesis is possible; $KCu(L^2)_2$ is also produced by reaction of KL^2 with $(CuL^2)_3$. Reaction of $Cu(L^2)_2$ with Cp_2Co proceeds in high yield to form $Cu(L^2)_2^-$. Reaction of $(CuOTf)_2{\cdot}C_6H_6$ with 4 KL^2 in C_6D_6 yields $KCu(L^2)_2$ together with a small amount of trimer $(CuL^2)_3$. However, there is no reaction between $Cu(L^2)_2$ and KL^2; $Cu(L^2)_2$ is thus not Lewis acidic toward this bidentate ligand, which is why we observe no chelate ligand redistribution for divalent copper.

DISCUSSION

The nonredox reactivity of $M(L^2)_2$ species here is in accord with the fact that electron withdrawing CF_3 groups increase the Lewis acidity of metal complexes.[23] However, as the number of d electrons increases, even this effect can be defeated: formation of 5-coordinate species from $M(L^2)_2$ follows the order Fe > Co > Ni > Cu. Thus, as the number of d electrons increases, Lewis acidity decreases. While we established this trend with THF, it is interesting that even bidentate $(L^2)^{1-}$ can bind to $M(L^2)_2$ for M = Fe, Co, and Ni. It is clear, from comparison of addition to $Fe(L^2)_2$ by either L^{1-} (paramagnetic product) or 2 CO (diamagnetic product), that the d orbital splitting is much larger when two strong π acid carbonyls add, yielding a low spin molecule.

Structural details of *mer*-$M(L^2)_3^{-1}$ show that, for a given metal, the pyrrolide at the center of the T of the *mer* shape always has the longer M−N distance. Since this pyrrolide is η^5-

dx.doi.org/10.1021/ic400803e | Inorg. Chem. 2013, 52, 5611−5619

coordinated to K^+, it appears that this leaves that pyrrolide less nucleophilic, hence with a longer bond to metal. This lengthening, together with the electron withdrawing effect of CF_3 substituents, diminishing the nucleophilicity of L^2 anion, perhaps facilitates chelate loss from a transition metal, hence the redistribution observed here; if true, this means that the more nucleophilic ^{t}Bu substituted pyridylpyrrolides may be more resistant to such redistribution, following reduction.

Since the magnetic susceptibility determination for $KFe(L^2)_3$ shows both z^2 and $x^2 - y^2$ to be singly occupied, it is likely to be also true for d^7 cobalt case, and thus, no *significant* (based on the σ bonding orbitals) Jahn–Teller effect is expected to distinguish, structurally, iron from cobalt here.

CONCLUSION

The surprise from this work is that this was intended as a reduction reaction but the characterized product is still divalent metal for Fe, Co, and Ni. The product described above is one of ligand redistribution. We conclude that the reaction is disproportionation ($3\ ML_2 + 2\ K \rightarrow 2\ KML_3 + M$) and have indeed detected metal particles by powder X-ray diffraction and EDX. We consider (Scheme 2) that the reaction begins from

Scheme 2. Proposed Mechanism[a]

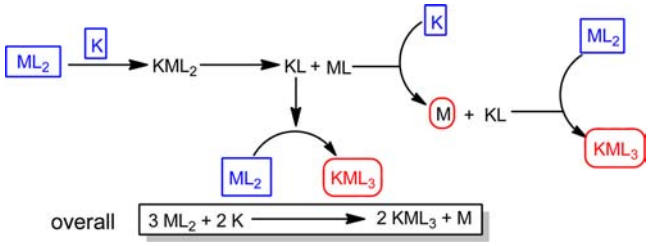

[a]Reactants in blue boxes; products in red ovals.

one electron reduction, forming in fact $KM(L^2)_2$, and that additional reduction of this is slower than loss of KL (which will add to ML_2 to make one mole of product KML_3), yielding the highly unsaturated ML. This we propose will be reduced by additional K to yield bulk metal and KL. The fact that ML_2 was shown independently to react with KL to give KML_3 confirms both the unsaturation of ML_2, and the viability of this as a mechanistic step. But overall the $3M(II) + 2K \rightarrow 2M(II) + M(0) + 2\ K^+$ electron balance shows that it is a shortage of ligands which leads to formation of bulk metal. In addition, anion L^2 is more likely to be released (as KL^2), given its two electron withdrawing substituents and thus its lowest nucleophilicity among other pyridylpyrrolides.[10]

In terms of our original goal of isolating species of formula $M(L^2)_2^{1-}$, while these are apparently formed, judging by CV as well as by the reactions in Scheme 2, these are only transients on the way to other products favored under these reactive conditions. The hypothesis that these follow-up reactions are caused by electrophilic cations (Na^+ or K^+) finds no support since outer sphere electron transfer reduction, leaving Cp_2Co^+ as the (inert) counterion, still shows chelate ligand redistribution. Attempts to capture $Fe(L^2)_2^{1-}$ with 1 atm N_2, CO_2, or H_2 all fail to outrun the ligand redistribution reaction.

EXPERIMENTAL SECTION

General Procedures. All manipulations were carried out under an atmosphere of purified nitrogen using standard Schlenk techniques or in a glovebox. Solvents were purchased from commercial sources, purified either using an Innovative Technology SPS-400 PureSolv solvent system or by distilling from conventional drying agents and degassed by the freeze–pump–thaw method twice prior to use or by activated alumina and Q-5 deoxygenation columns. Glassware was oven-dried at 150 °C overnight. NMR spectra were recorded in C_6D_6 or D-8 THF at 25 °C on a Varian Inova-400 spectrometer (^{1}H, 400.11 MHz; ^{13}C, 100.61 MHz; ^{19}F, 376.48 MHz) or on a 300 MHz spectrometer. Proton and carbon chemical shifts are reported in ppm versus Me_4Si; ^{19}F NMR chemical shifts are referenced relative to external CF_3CO_2H. Mass spectrometry analyses were performed in an Agilent 6130 MSD (Agilent Technologies, Santa Clara, CA) quadrupole mass spectrometer equipped with a Multimode (ESI and APCI) source. High resolution mass spectra were obtained on a ThermoFinnigan MAT95XP mass spectrometer. Electrochemical studies were carried out with an Autolab model PGSTAT30 potentiostat (Eco Chemie). A three-electrode configuration consisting of a working electrode (platinum button electrode for Co but glassy carbon for Fe and Ni), $Ag/AgNO_3$ (0.01 M in MeCN with 0.1 M n-Bu_4NPF_6) reference electrode, and a platinum coil counter electrode was used. All electrochemical potentials were referenced with respect to the Cp_2Fe/Cp_2Fe^+ redox couple, added internally with the sample at the end of a study. The CV of $Fe(L^2)_2$ was measured in THF at both Pt and glassy carbon electrodes, and reduction is 200 mV easier at the Pt-electrode and oxidation becomes irreversible. Magnetic susceptibilities were measured in a concentric NMR tube, using hexamethylbenzene as internal standard. Potassium graphitate, KC_8, was made by a literature method.[24] The synthesis of HL^2 has been described.[9] EDX data were collected on a JEOL JEM 3200FS equipped for STEM and with an Oxford INCA EDX system. Elemental analysis were performed at Robertson Microlit Laboratories.

Synthesis of $[Fe(L^2)_2(THF)]$. A 100 mg of portion of L^2H (1 equiv, 0.36 mmol) in 20 mL of THF was slowly added to the stirring mixture of 15.0 mg of KH (1.05 equiv., 0.37 mmol) in 20 mL of THF. After 1 h, gas evolution had ended, and full conversion into L^2K was observed. The solution was filtered through a Celite plug and used without further purification. A 22.8 mg portion of anhydrous $FeCl_2$ (0.18 mmol, 0.50 equiv) was added to the stirring solution of L^2K, and the reaction mixture was stirred under argon at RT for 18 h. The initial colorless solution became orange after 2 h and then finally yellow. After removal of solvent under reduced pressure, the yellow solid residue was dissolved in 10 mL of benzene, the resulting yellow solution was filtered through Celite, and the solvent was removed under reduced pressure. The yellow solid thus obtained was collected and washed with 5 × 2 mL of pentane, and then dried under vacuum for 4 h at 25 °C. Evaporation of solvent under reduced pressure yielded the pure yellow solid compound. Crystals suitable for X-ray analysis were obtained by slow evaporation of a saturated pentane solution at room temperature under argon atmosphere. Isolated yield: 223 mg (91%). ^{1}H NMR (D-8 THF, 25 °C): δ = −4.43 (br, 1H), 52.24 (br, 1H), 74.02 (br, 1H), 78.15 (br, 1H), 89.10 (br, 1H). ^{19}F NMR /(D-8 THF, 25 °C): −75.25 (s), −6.28 (s). ^{1}H NMR (C_6D_6, 25 °C): −18.16 (br, 1H), 10.15 (br, 2H, THF), 21.01 (br, 2H, THF), 50.92 (br, 1H), 72.64 (br, 1H), 73.56 (br, 1H), 82.52 (br, 1H). ^{19}F NMR (C_6D_6 + 10% THF, 25 °C): −55.34 (s), −7.74 (s). MS (APCI-negative ion, in THF). Calcd (Found) for $[M(L^2)_3]^-$: m/z 893.3 (893.3). Multiple attempts to get satisfactory elemental analysis gave consistently low values for carbon, even with use of V_2O_5 combustion promoter, which we attribute to formation of refractory iron carbide. Anal. Calcd for $Fe(L^2)_2(THF)$, $C_{26}H_{18}F_{12}FeN_4O$: C, 45.50; H, 2.64; N, 8.16. Found: C, 43.34; H, 2.15; N, 7.83.

Removal of THF from $[Fe(L^2)_2(THF)]$. Several attempts were made to remove the coordinated THF from $Fe(L^2)_2(THF)$. The yellow solid $Fe(L^2)_2THF$ was dissolved in a minimum volume of benzene and pumped to dryness four times; no significant color change was observed. Treatment of solid $Fe(L^2)_2(THF)$ with vacuum at 45 °C produced degradation of solid $Fe(L^2)_2(THF)$ to numerous uncharacterized products. However, vacuum treatment for 24 h at 25 °C gave a clean conversion to a pale red compound which retains one THF molecule for each two Fe atoms. Longer time in vacuum does

dx.doi.org/10.1021/ic400803e | Inorg. Chem. 2013, 52, 5611–5619

not lead to full conversion to $Fe(L^2)_2$, and vacuum treatment at 45 °C leads to decomposition to multiple products. ^{1}H NMR (C_6D_6, 25 °C): −12.60 (br, 1H), 27.19 (br, 1H, THF), 49.34 (br, 1H), 55.17 (br, 1H, THF), 78.57 (br, 1H), 80.56 (br, 1H), 84.79 (br, 1H). ^{19}F NMR (C_6D_6 + 10% THF, 25 °C): 2.20 (s), 5.62 (s).

Reaction of KC_8 with $[Fe(L^2)_2(THF)]$: $[KFe(L^2)_3]$. A 25 mg portion of $Fe(L^2)_2(THF)$ (1 equiv, 0.015 mmol) was dissolved in 5 mL of THF solution under argon. A 12.33 mg portion of KC_8 (2.2 equiv, 0.033 mmol) was added into that solution. The initial yellow solution became green and then finally an orange-red color. After 3 h full conversion into a single product was confirmed by monitoring the reaction by ^{1}H NMR and ^{19}F NMR. The solution was filtered through a Celite plug, and the solvent was removed under reduced pressure. The orange solid thus obtained was collected and dried under reduced pressure. Crystals suitable for X-ray analysis were obtained from a saturated solution of toluene at −35 °C and identified as $KFe(L^2)_3$. The same reaction was carried out in different conditions by changing atmosphere (N_2, CO_2, and H_2), solvent (THF and Et_2O), and reductant (2.2 equiv elemental Na) (see Supporting Information). In all cases (see Supporting Information for details) the only soluble product was $KFe(L^2)_3$; however, in the case of K under H_2 10−15% $(L_2)K$ was obtained as a side product. ^{1}H NMR (D-8 THF, 25 °C): δ 13.18 (br, 1H), 18.16 (br, 1H), 38.18 (br, 1H), 39.96 (br, 1H), 50.56 (br, 1H), 60.38 (br, 2H), 61.70 (br, 1H), 68.77 (br, 1H), 70.14 (br, 1H), 70.46 (br, 1H), 73.03 (br, 1H), 83.60 (br, 1H), 141.50 (br, 1H). The fifteenth proton is presumably too broad to detect. ^{19}F NMR (D-8 THF, 25 °C): δ −105.74 (s), −96.74 (s), −96.35 (s), −23.44 (s), −14.98 (s), 11.08 (s). We examined the graphite fraction after our reaction for evidence of production of iron. Powder X-ray diffraction showed several lines for FeO (broad, consistent with small particle size), which we interpret as oxidation of highly reactive iron particles during diffraction sample preparation and data collection. We also collected energy dispersive X-ray spectroscopy data of particles visualized in an electron microscope. These showed confirmatory evidence for iron in a number of the graphite particles investigated. Also seen in the EDX data were K and Cl, which we attribute to KCl formed when the microscopic sample preparation solvent, CH_2Cl_2, contacts residual potassium in the KC_8. A control experiment (KC_8 with sample transfer to grid with CH_2Cl_2) was also done to confirm that the additional Cl peak in EDX originated from the CH_2Cl_2 in presence of a strong reductant.

Reaction of $[Fe(L^2)_2(THF)]$ with CO: $[Fe(L^2)_2(CO)_2]$. A 10 mg portion of $Fe(L^2)_2(THF)$ (0.015 mmol, 1 equiv) was placed in an NMR tube and dissolved in 0.5 mL of C_6D_6. An excess of CO gas (1 atm.) was added by standard gas addition techniques. No significant color change was observed immediately; however, it finally changed to deep yellow from yellow. The reaction was complete within an hour, showing a complete consumption of starting material followed by formation of only one new diamagnetic compound. Applying vacuum for 3−4 h does not reconvert to the starting material or cause loss of any CO. ^{1}H and ^{19}F NMR were taken; a free THF signal in the ^{1}H NMR proves that CO successfully replaces the coordinated THF. Volatiles were removed under reduced pressure followed by additional 1 h more vacuum to remove the generated free THF. The yellow solid thus obtained was dissolved in CD_2Cl_2, and NMR was taken again. ^{1}H NMR (C_6D_6, 25 °C): δ 1.42 (br, 2H, THF), 3.57 (br, 2H, THF), 5.80 (t, J = 6.57, 6.24, 1H), 6.44 (t, J = 7.67, 7.56, 1H), 6.56 (d, J = 5.56, 1H), 7.65 (d, J = 8.2, 1H). (The fifth ring signal is merged with the residual C_6H_6 peak.) ^{19}F NMR (C_6D_6, 25 °C): δ −55.59 (s), −57.16 (s). ^{1}H NMR (CD_2Cl_2, 25 °C): δ = 6.72 (d, J = 5.7, 1H), 7.05 (t, J = 6.45, 6.52, 1H), 7.11 (s, 1H), 7.79 (t, J = 7.55, 8.34, 1H), 7.91 (d, J = 8.25, 1H). IR: ν_{CO} (solid KCl disk) = 2088 and 2044 cm^{-1}. MS (MALDI) negative ion chemical ionization calcd (found) for $[M - CO]^-$: m/z: 642.001 (642.004)and $[M - 2CO]^-$: m/z 614.006 (614.002). Positive ion chemical ionization calcd (found) for $[M - 2CO]^+$: m/z 614.006 (614.002).

Synthesis of $[Co(L^2)_2]$. A 128.1 mg (0.402 mmol) portion of KL^2 and 27.2 mg (0.209 mmol) of $CoCl_2$ were added to 15 mL of THF. Upon addition the solution was a greenish-brown and after 24 h of mixing the solution became a dark green color, which was then filtered through Celite. A mixture of dark-brown and green solids are obtained upon removal of the solvent under reduced pressure. The solids were dissolved in 5 mL of benzene and pumped to dryness to remove coordinated THF. This procedure was performed three times to ensue removal of adventitious THF. The resulting brown-red solid was then dissolved in 5 mL of benzene and filtered through Celite. The filtrate was dried under reduced pressure, yielding a brownish-red solid. The solid was obtained in 66% yield. Single crystals were grown by cooling a saturated toluene solution to −35 °C. ^{1}H NMR (C_6D_6, 25 °C): δ 143.2 (br, 1H), 106.1 (br, 1H), 30.6 (br, 1H), 11.9 (br, 1H), 2.2 (br, 1H). ^{19}F NMR (C_6D_6, 25 °C): δ66.4 (s), −52.0 (s). MS (APCI, positive): 617.0; $C_{22}H_{10}CoF_{12}N_4$ Calcd 617.0. MS (APCI, negative): found, 896.1; $C_{33}H_{15}CoF_{18}N_6$ calcd 896.0. Magnetic moment in solution (Evans method; hexamethylbenzene as reference): μ_{eff} = 4.20 μ_B. Anal. Calcd for $Co(L^2)_2$(toluene), $C_{29}H_{18}CoF_{12}N_4$: C, 49.10; H, 2.56; N, 7.90. Found: C, 48.94; H, 2.57; N, 7.86.

Reaction of $[Co(L^2)_2]$ with THF: $[Co(L^2)_2(THF)]$. A 10.2 mg (0.017 mmol) portion of brownish-red $Co(L^2)_2$ was dissolved in 0.3 mL of D-8 THF in a J. Young NMR tube yielding a green solution upon dissolving. Full conversion of $Co(L^2)_2$ to the solvated $Co(L^2)_2(THF)$ occurred instantaneously upon adding THF which was characterized by NMR spectroscopy. Low temperature ^{1}H NMR spectra at −50 °C could not resolve signals for coordinated and free THF. Removal of solvent under reduced pressure results in conversion back to $Co(L^2)_2$. No attempts were made to isolate the adduct. ^{1}H NMR (D-8 THF, 25 °C): δ 108.8 (br, 1H), 83.9 (br, 1H), 73.6 (br, 1H), 41.3 (br, 1H), −0.9 (br, 1H). ^{19}F NMR (D-8 THF, 25 °C): δ −9.3 (s), −77.7 (s).

Reaction of $[Co(L^2)_2]$ with Benzonitrile: $[Co(L^2)_2$(benzonitrile)]. A 19.8 mg (0.032 mmol) portion of brownish-red $Co(L^2)_2$ was dissolved in 0.3 mL of C_6D_6 in a J. Young NMR tube yielding a brownish red solution. A 0.1 mL portion of benzonitrile (0.970 mmol) was added to the solution resulting in a color change from red-brown to green immediately upon addition. Full conversion to the $Co(L^2)_2$(NCPh) adduct was characterized by NMR spectroscopy. Multiple aromatic signals for free benzonitrile and coordinated benzonitrile overlapped in the ^{1}H NMR spectrum and could not be resolved. No attempts were made to isolate the adduct. ^{1}H NMR (C_6D_6, 25 °C): δ 118.0 (br, 1H), 83.0 (br, 1H), 57.5 (br, 1H), 36.7 (br, 1H), −0.0 (br, 1H). ^{19}F NMR (C_6D_6, 25 °C): δ −11.0 (s), −78.2 (s).

Synthesis of Complex $[KCo(L^2)_3]$·(Toluene). *Method A.* A 11.3 mg (0.030 mmol) portion of KC_8 suspended in 1 mL C_6D_6 was added dropwise to 8.2 mg (0.013 mmol) of $Co(L^2)_2$ dissolved in 0.5 mL of C_6D_6. The red-brown solution immediately darkened in color to brown. After 30 min of mixing the reaction mixture was filtered through Celite to remove the graphite, yielding a yellow solution. Full conversion to $[K(toluene)][Co(L^2)_3]$ was characterized by NMR spectroscopy. Attempts to isolate the product as a powder by removal of solvent under reduced pressure results in KL^2 and $Co(L^2)_2$. To obtain single crystals of $[K(toluene)][Co(L^2)_3]$ the above reaction had to be performed in toluene using similar concentrations. After filtering the reaction mixture through Celite to remove graphite, 5 drops of pentane were added to the toluene solution, and the reaction mixture was cooled to −35 °C resulting in the formation of single crystals. Energy dispersive X-ray spectroscopy data of the filtered graphite was visualized in an electron microscope. These showed confirmatory evidence for cobalt mixed with the graphite particles separated during the reaction workup. Also seen in the EDX mixed with graphite was potassium, which we attribute to residual KC_8 or KCl generated during sample preparation using CH_2Cl_2. ^{1}H NMR (C_6D_6, 25 °C): δ 115.9 (br, 1H), 108.5 (br, 1H), 91.5 (br, 1H), 71.2 (br, 1H), 70.9 (br, 1H), 54.6 (br, 1H), 41.5 (br, 1H), 33.6 (br, 1H), 22.6 (br, 1H), 11.3 (br, 1H), 7.8 (br, 1H), 4.2 (br. 1H), 4.0 (br, 1H) 1.67 (br, 1H). ^{19}F NMR (C_6D_6, 25 °C): δ −18.6 (s), −21.6 (s), −24.9 (s), −69.6 (s), −92.4 (s), −118.5 (s).

Method B. A 8.2 mg (0.063 mmol) portion of $CoCl_2$ was dissolved in 5 mL of THF yielding a blue solution. The $CoCl_2$ solution was added dropwise to a yellow THF solution of 58.6 mg (0.184 mmol) of KL^2. The solution maintained a yellow color, and after mixing for 3 h

dx.doi.org/10.1021/ic400803e | Inorg. Chem. 2013, 52, 5611−5619

the reaction mixture was filtered through Celite. Full conversion to $[KCo(L^2)_3]$ was monitored by ^{19}F NMR spectroscopy. All fluorine signals were consistent with the product obtained from method A.

Synthesis of $Ni(L^2)_2(THF)$. A 100 mg portion of L^2H (0.357 mmol) in 10 mL of THF was slowly added to the stirring mixture of 15.0 mg of KH (1.05 equiv, 0.374 mmol) in 10 mL of THF. After 30 min gas evolution had ended, and full conversion into L^2K was observed. A 32.1 mg portion of $NiCl_2(THF)_{0.7}$ (0.178 mmol) was added to the stirring solution of L^2K. After 12 h of vigorous stirring at 60 °C, all volatiles were removed from light yellow-green solution in vacuum, the residue was treated with 20 mL of benzene, solid KCl was filtered off, and the light yellow solution was dried in vacuum (0.1 mm Hg) for 1 h to give a pale green powder of $(L^2)_2Ni(THF)$. ^1H NMR (THF D-8, 25 °C): 11.89 (br, 2H), 50.81 (br, 2H), 55.19 (br, 2H), 98.33 (br, 2H), 159.42 (br, 2H). ^{19}F NMR (THF D-8, −20 °C): −70.5 (s), −41.2 (s). ^{19}F NMR (THF D-8, 25 °C): −52.6 (s), −42.5 (s). MS (APCI-negative ion, THF) expt 616.0 $C_{22}H_{10}F_{12}N_4Ni$ or $[M - C_4H_8O]^-$. Calcd: 616.0067; no ion was seen under typical conditions in the positive ion mode AP CI scans.

Synthesis of $KNi(L^2)_3$ by Reaction of $Ni(L^2)_2(THF)$ with KL^2. KL^2 (7.3 mg, 0.023 mmol) was added to a light green solution of $NiL^2_2(THF)$ (15.4 mg, 0.022 mmol) in THF at room temperature. Upon mixing the solution turned a pale yellow color with the formation of $KNiL^2_3$, which shows six signals in the ^{19}F NMR spectrum and at least 12 signals in the ^1H NMR spectrum. Reaction of NiL^2_2 with KC_8, sodium metal, or $CoCp_2$ in THF or benzene gave wholly equivalent results. ^1H NMR (D-8 THF, 25 °C): δ 12.3 (br, 1H), 13.9 (br, 1H), 14.5 (br, 1H), 44.2 (br, 1H), 45.9 (br, 1H), 47.0 (br, 1H), 47.8 (br, 1H), 49.2 (br, 2H), 79.2 (br, 1H), 87.4 (br, 1H), 89.1 (br, 1H). The last three peaks are presumably too broad to detect. ^{19}F NMR (D-8 THF, 25 °C): δ −76.4 (s), −74.8 (s), −71.7 (s), −43.0 (s), −42.5 (s), −42.2 (s). Magnetic susceptibility, using the Evans method in concentric NMR tubes, by monitoring the ^1H NMR shift of reference hexamethylbenzene in C_6D_6 at 25 °C yielded a value of 2.74 μ_B, corresponding to two unpaired electrons.

Synthesis of $KCu(L^2)_2$ by Reaction of $(CuL^2)_3$ with $3KL^2$. $(CuL^2)_3$[9] (15 mg, 0.0146 mmol) was dissolved in 0.5 mL of deuterated benzene at room temperature to form a light yellow solution. Three equivalents of colorless KL^2 (15.3 mg, 0.0482 mmol, 10% excess) in 0.5 mL benzene was added dropwise to the copper complex solution. Upon mixing, the solution turned a dark yellow-orange color with full conversion to product. The solution was filtered through Celite and dried in vacuo to form a yellow-orange solid. ^1H NMR (C_6D_6, 25 °C): δ 6.38 (t, J = 6.4, 1H, C−H Ar), 7.04 (t, J = 7.6, 1H, C−H Ar), 7.33 (s, 1H, C−H pyrrole), 7.86 (d, J = 4.4, 1H, C−H Ar), 8.12 (d, J = 8, 1H, C−Ar). ^{19}F NMR (C_6D_6, 25 °C): δ −58.16 (s), −53.68 (s). The product of the reaction of 1:1.25 mol ratio of $Cu(L^2)_2$ and KC_8 in C_6D_6 is identical according to ^1H and ^{19}F NMR spectroscopy, though the lines are broadened such that the J couplings cannot be observed (see text). A similar product is also observed by NMR when $(CuL^2)_3$ reacts with cobaltocene, though the color of the product is dark red, and the doublet at 7.86 ppm in the ^1H NMR is shifted downfield to 8.06 ppm, with the J value decreased to 1.1 Hz. ^1H NMR (C_6D_6, 25 °C): δ 6.38 (t, J = 6.4, 1H, C−H Ar), 7.05 (t, J = 7.6, 1H, C−H Ar), 7.35 (s, 1H, C−H pyrrole), 8.06 (d, J = 1.1, 1H, C−H Ar), 8.10 (d, J = 8, 1H, C−Ar). ^{19}F NMR (C_6D_6, 25 °C): δ −58.71 (s), −52.96 (s). We attribute these subtle spectroscopic changes to ion pairing of Cp_2Co^+ with $Cu(I)(L^2)_2^-$, influenced by the ring current effect of nearby cyclopentadienyl ring. The presence of Cp_2Co also moves the chemical shift of electron transfer product Cp_2Co^+ due to rapid electron exchange with trace paramagnetic Cp_2Co. In general, NMR spectra of samples of $KCu(L^2)_2$ derived from reductive synthetic paths often have less resolution of spin/spin splitting among the pyridyl protons due to residual trace amounts of paramagnetic impurities, such as Cp_2Co. Likewise, samples of diamagnetic $Cu(L^2)_2^{1-}$ sometimes have broadened signals due to fast outer sphere electron transfer with trace residual paramagnetic $Cu(L^2)_2$. MS (APCI, negative): 279.1, $C_{11}H_5F_6N_2$ Calcd 279.0; 621.0; $C_{22}H_{10}CuF_{12}N_4$ Calcd 621.0; when the injector contains oxidizing chlorocarbons, e.g., CH_2Cl_2, one also observes $Cu(L^2)_2Cl^{1-}$ from oxidation of monovalent copper anionic complexes.

■ ASSOCIATED CONTENT

Ⓢ Supporting Information

Additional figures, tables, and details. This material is available free of charge via the Internet at http://pubs.acs.org.

■ AUTHOR INFORMATION

Corresponding Author

*E-mail: caulton@indiana.edu.

Notes

The authors declare no competing financial interest.

■ ACKNOWLEDGMENTS

This work was supported by the National Science Foundation.

■ REFERENCES

(1) Broudy, P. M.; Berry, A. D.; Wayland, B. B.; MacDiarmid, A. G. *J. Am. Chem. Soc.* **1972**, *94*, 7577.

(2) Chisholm, M. H.; Huffman, J. C.; Rothwell, I. P.; Bradley, P. G.; Kress, N.; Woodruff, W. H. *J. Am. Chem. Soc.* **1981**, *103*, 4945.

(3) Chisholm, M. H.; Kober, E. M.; Ironmonger, D. J.; Thornton, P. *Polyhedron* **1985**, *4*, 1869.

(4) Echegoyen, L.; Perez-Cordero, E.; Regnouf de Vains, J. B.; Roth, C.; Lehn, J. M. *Inorg. Chem.* **1993**, *32*, 572.

(5) Kraft, S. J.; Fanwick, P. E.; Bart Suzanne, C. *Inorg. Chem.* **2010**, *49*, 1103.

(6) Perez-Cordero, E.; Buigas, R.; Brady, N.; Echegoyen, L.; Arana, C.; Lehn, J. M. *Helv. Chim. Acta* **1994**, *77*, 1222.

(7) Perez-Cordero, E. E.; Campana, C.; Echegoyen, L. *Angew. Chem., Int. Ed.* **1997**, *36*, 137.

(8) Wagner, M. J.; Dye, J. L.; Perez-Cordero, E.; Buigas, R.; Echegoyen, L. *J. Am. Chem. Soc.* **1995**, *117*, 1318.

(9) Andino, J. G.; Flores, J. A.; Karty, J. A.; Massa, J. P.; Park, H.; Tsvetkov, N. P.; Wolfe, R. J.; Caulton, K. G. *Inorg. Chem.* **2010**, *49*, 7626.

(10) Flores, J. A.; Andino, J. G.; Tsvetkov, N. P.; Pink, M.; Wolfe, R. J.; Head, A. R.; Lichtenberger, D. L.; Massa, J.; Caulton, K. G. *Inorg. Chem.* **2011**, *50*, 8121.

(11) Rose, R. P.; Jones, C.; Schulten, C.; Aldridge, S.; Stasch, A. *Chem.—Eur. J.* **2008**, *14*, 8477.

(12) See Supporting Information.

(13) Cotton, F. A.; McCleverty, J. A. *Inorg. Chem.* **1964**, *3*, 1398.

(14) Vendemiati, B.; Prini, G.; Meetsma, A.; Hessen, B.; Teuben, J. H.; Traverso, O. *Eur. J. Inorg. Chem.* **2001**, 707.

(15) Chambers, J.; Eaves, B.; Parker, D.; Claxton, R.; Ray, P. S.; Slattery, S. J. *Inorg. Chim. Acta* **2006**, *359*, 2400.

(16) Jie, S.; Agostinho, M.; Kermagoret, A.; Cazin, C. S. J.; Braunstein, P. *Dalton Trans.* **2007**, 4472.

(17) Kruck, M.; Sauer, D. C.; Enders, M.; Wadepohl, H.; Gade, L. H. *Dalton Trans.* **2011**, *40*, 10406.

(18) Athimoolam, A.; Gambarotta, S.; Korobkov, I. *Can. J. Chem.* **2005**, *83*, 832.

(19) Ganesan, M.; Berube, C. D.; Gambarotta, S.; Yap, G. P. A. *Organometallics* **2002**, *21*, 1707.

(20) Ilango, S.; Vidjayacoumar, B.; Gambarotta, S. *Dalton Trans.* **2010**, *39*, 6853.

(21) Ilango, S.; Vidjayacoumar, B.; Gambarotta, S.; Gorelsky, S. I. *Inorg. Chem.* **2008**, *47*, 3265.

(22) Scott, J.; Gambarotta, S.; Yap, G. P. A.; Rancourt, D. G. *Organometallics* **2003**, *22*, 2325.

(23) Siedle, A. R.; Pignolet, L. H. *Inorg. Chem.* **1982**, *21*, 135.

(24) Schwindt, M. A.; Lejon, T.; Hegedus, L. S. *Organometallics* **1990**, *9*, 2814.